The 59-kD protein was a minor protein in the cell wall (Fig. 2). The low protein number and the low specific activity of the channel were in good agreement with the low permeability of the cell wall of *M. chelonae*, as measured by the liposome swelling assay (the specific activity of the cell wall was 0.54 for arabinose) or measured in intact cells (5). The permeability of the cell wall of *M. chelonae* was significantly lower than that of the outer membranes of the Gram-negative bacteria *P. aeruginosa* and *Escherichia coli* (5).

To test whether the crude cell wall extracts and the purified 59-kD protein of the cell wall formed defined channels or simply represented an undefined leakage pathway, we performed single-channel experiments with lipid bilayer membranes (13). Addition of small amounts of the cell wall or of the pure 59-kD protein (final concentrations, 1 to 10 ng/ml) to the aqueous solution in contact with a lipid bilayer membrane caused the formation of ion-permeable channels (Fig. 3). These channels could only have been present in the cell wall because their presence in the cytoplasmic membrane would have resulted in the death of the cell. The channels were mostly stable and occasionally showed a fast flickering between a closed and an open state (Fig. 3). The average single-channel conductance was 2.7 nS in 1 M KCl, which is larger than those found with porins of enteric bacteria (14). The single-channel conductance could also be used to generate a rough estimate of the channel size (13). If we assume that the lipid layer has a thickness of 12 nm (15), the channel size would be approximately 1.9 nm. This value has to be considered an approximation because we do not know the exact length of the lipid layer and because we may be dealing with a specialized channel such as the specific porins of Gram-negative bacteria (14). The results from the liposome swelling assays and from the lipid bilayer experiments suggest that our picture of a defined hydrophilic pathway formed by the 59-kD protein was correct. The 59-kD protein would act as a mycobacterial porin and form the necessary channels for the diffusion of nutrients into the cell and of waste products to the environment. Better knowledge of this system could help improve antibiotic design to overcome the permeability barrier of the cell-wall lipid layer of mycobacteria.

REFERENCES AND NOTES

1. Joint International Union Against Tuberculosis and World Health Organization Study Group, *Tubercle* **63**, 157 (1982).
2. B. R. Bloom, *Nature* **342**, 115 (1989).
3. C. R. Horsburgh, *N. Engl. J. Med.* **324**, 1332 (1991).
4. P. F. Barnes, A. B. Bloch, P. T. Davidson, D. E. Snider, *ibid.*, p. 1644.
5. V. Jarlier and H. Nikaido, *J. Bacteriol.* **172**, 1418 (1990).
6. J. Jarlier, L. Gutmann, H. Nikaido, *Antimicrob. Agents Chemother.* **35**, 1937 (1991).
7. P. J. Wheeler and C. Ratledge, *Br. Med. Bull.* **44**, 547 (1988).
8. D. E. Minnikin, in *Chemotherapy of Tropical Diseases*, M. Hooper, Ed. (Wiley, Chichester, England, 1987), pp. 19–43.
9. H. Nikaido, K. Nikaido, S. Harayama, *J. Biol. Chem.* **266**, 770 (1991).
10. H. Nikaido and E. Y. Rosenberg, *J. Gen. Physiol.* **77**, 121 (1981).
11. J. Trias and R. Benz, in preparation.
12. F. Yoshimura, L. S. Zalman, H. Nikaido, *J. Biol. Chem.* **258**, 2308 (1983).
13. R. Benz, K. Janko, W. Boos, P. Lauger, *Biochim. Biophys. Acta* **511**, 305 (1978).
14. R. Benz, *Annu. Rev. Microbiol.* **42**, 359 (1988).
15. P. Draper, in *The Biology of Mycobacteria*, T. Ratledge and J. Stanford, Eds. (Academic Press, London, 1982), pp. 9–52.
16. *Mycobacterium chelonae* PS4770 was used for all the experiments and grown as described in (5). Cell suspensions were broken by homogenization with microglass beads by a Homogenisator MSK (B. Braun Biotech) according to the manufacturer's instruction. The homogenized sample was then centrifuged at 3,000 rpm for 10 min and the supernatant was collected and pelleted at 20,000 rpm for 30 min to obtain the cell envelopes (cell wall and cytoplasmic membrane). The cell wall was purified by sucrose-gradient centrifugation in a modification of the method of Hirschfield and colleagues (17). The pellet was suspended in 1 ml and applied to a step sucrose gradient of 30, 40, and 70% sucrose (w/v). The fraction containing the cell wall, between 40 and 70%, was centrifuged and the pellet was washed twice and used as cell wall fraction. This fraction was essentially free of cytoplasmic membrane as assessed by reduced nicotinamide adenine dinucleotide (NADH) oxidation; at this point only 0.1% of total NADH activity was associated with this fraction. The cell wall fraction was washed once by centrifugation with a buffer containing 20 mM tris-HCl (pH 8), 1% Zwittergent 3-12 (Calbiochem), and 3 mM NaN_3, and proteins were extracted with a solution containing the same buffer solution supplemented with 40 mM EDTA. After 1 hour of incubation at room temperature, the solution was centrifuged and the supernatant was collected. After dialysis, the cell wall extracts (20 μg) were incubated with 0.1 μg of Pronase (Boehringer Mannheim) or protease K (Sigma) for 5 hours at 37°C according to the manufacturer's instructions. Liposomes were reconstituted with 10 μg of protein after extensive dialysis against distilled water, and swelling rates were determined as in Fig. 2 and normalized to the untreated control rate. Control liposomes with Pronase or protease K were also reconstituted and did not show any significant swelling. Data represent the average of three experiments; standard errors are in brackets.
17. G. R. Hirschfield, M. McNeil, P. J. Brennan, *J. Bacteriol.* **172**, 1005 (1990).

18. Supported by a grant from the United Nations Development Programme–World Bank–World Health Organization Programme for Research and Training in Tropical Diseases and at the University of Wurzburg by the Deutsche Forschungsgemeinschaft (project B9 of the Sonderforschungsbereich 176) and the Fonds der Chemischen Industrie. We thank A. Schmid for helpful discussions.

10 March 1992; accepted 9 September 1992

Antisense and Antigene Properties of Peptide Nucleic Acids

Jeffery C. Hanvey, Nancy J. Peffer, John E. Bisi, Stephen A. Thomson, Rodolfo Cadilla, John A. Josey, Daniel J. Ricca, C. Fred Hassman, Michele A. Bonham, Karin G. Au, Stephen G. Carter, David A. Bruckenstein, Ann L. Boyd, Stewart A. Noble, Lee E. Babiss*

Peptide nucleic acids (PNAs) are polyamide oligomers that can strand invade duplex DNA, causing displacement of one DNA strand and formation of a D-loop. Binding of either a T_{10} PNA or a mixed sequence 15-mer PNA to the transcribed strand of a G-free transcription cassette caused 90 to 100 percent site-specific termination of pol II transcription elongation. When a T_{10} PNA was bound on the nontranscribed strand, site-specific inhibition never exceeded 50 percent. Binding of PNAs to RNA resulted in site-specific termination of both reverse transcription and in vitro translation, precisely at the position of the PNA · RNA heteroduplex. Nuclear microinjection of cells constitutively expressing SV40 large T antigen (T Ag) with either a 15-mer or 20-mer PNA targeted to the T Ag messenger RNA suppressed T Ag expression. This effect was specific in that there was no reduction in β-galactosidase expression from a coinjected expression vector and no inhibition of T Ag expression after microinjection of a 10-mer PNA.

Sequence-specific binding of oligodeoxynucleotides (ODNs) to RNA or in the major groove of duplex DNA through triple-helix formation provides a way to modulate gene expression (1, 2). Although the potential of ODNs as antisense or antigene agents is actively being explored, the problems associated with creating in vivo bioefficacy and maintaining binding specificity and affinity are formidable.

J. C. Hanvey, N. J. Peffer, J. E. Bisi, S. A. Thomson, R. Cadilla, J. A. Josey, D. J. Ricca, C. F. Hassman, M. A. Bonham, K. G. Au, S. G. Carter, D. A. Bruckenstein, S. A. Noble, L. E. Babiss, Departments of Cell Biology and Medicinal Chemistry, Glaxo Inc. Research Institute, 5 Moore Drive, Research Triangle Park, NC 27709. A. L. Boyd, Department of Biology, Hood College, Frederick, MD 21701.

*To whom correspondence should be addressed.

Targeting of ODNs to DNA or RNA can block elongation of pol II transcription and reverse transcription (RT) in vitro (*3–5*). Young *et al.* (*3*) observed pausing of pol II transcription elongation at a triple helix, but efficient termination of transcription was only achieved by covalently cross-linking the ODN to the duplex DNA target (*3*). Boiziau *et al.* (*5*) demonstrated inhibition of RT with ODNs complementary to an RNA substrate. However, the inhibition of cDNA elongation resulted from cleavage at the RNA · ODN heteroduplex by the ribonuclease (RNase) H activity inherent in the reverse transcriptase (*5*). A similar requirement for RNase H has been described when ODNs have been used for translation arrest studies (*6*). In these examples, ODN–nucleic acid interactions alone were not sufficient to completely ablate polymerase or ribosome elongation.

An ODN analog in which the phosphodiester backbone was replaced with a polyamide (*7, 8*), termed a polyamide or peptide nucleic acid (PNA), has been shown to strand invade duplex DNA at a specific target site. Binding of a 10-mer PNA caused a local displacement of one of the two DNA strands (D-loop formation), as determined by sensitivity to single-strand specific agents (*7*). The strand displacement within duplex DNA was attributed to the high avidity of PNA for DNA; the melting temperature (T_m) for a complex of PNA T_{10} (with a terminal Lys amide) and dA_{10} was greater than 70°C (*8*). We now demonstrate in vitro site-specific termination of eukaryotic transcription at a PNA · DNA complex, site-specific termination of both RT and in vitro translation at a PNA · RNA complex, and in vivo sequence-specific inhibition of SV40 large T antigen (T Ag) expression.

We synthesized the PNA T_{10}Lys, a 10-mer homo-thymidine PNA containing a Lys amide group at its carboxyl terminus (Fig. 1A) (*9*). The physical interaction of this PNA with a plasmid (pBSA10) (*10*) containing a complementary $dA_{10} \cdot T_{10}$ target sequence was assayed with two experimental approaches. First, S1 nuclease was used qualitatively to scan for single-stranded regions within the DNA caused by PNA strand invasion. As observed by Nielsen *et al.* (*7*), we detected S1 nuclease hyperreactivity within a T_{10} segment but not within the complementary dA_{10} sequence (*11*) of pBSA10 in the presence of T_{10}Lys. However, S1 nuclease and the other chemical and enzymatic probes used by Nielsen *et al.* (*7*) are not effective for determining the percentage of DNA with PNA bound. We quantitated the extent of PNA strand invasion by measuring inhibition of Hind III cleavage at a site overlapping the target sequence for PNA binding. A similar assay has been used to measure binding of ODNs to duplex DNA through triple-helix formation (*2*).

The inhibition of Hind III cleavage caused by T_{10}Lys strand invasion at a site overlapping a $dA_{10} \cdot T_{10}$ sequence was determined with a 156-bp Bss HII–Kpn I restriction fragment of pBSA10 (*10*). This DNA fragment (Fig. 1B, lane 1) was incubated with varying doses of T_{10}Lys and then digested with Hind III (lanes 2 to 7) (*12*). Cleavage at the Hind III site in the absence of PNA strand invasion yielded an 86-bp radioactive fragment (lane 2), whereas PNA inhibition of Hind III cleavage at the PNA target site yielded a 110-bp radioactive fragment. A dose-dependent loss of the 86-bp fragment was observed with complete inhibition of Hind III cleavage at 0.8 μM PNA (~30:1 molar ratio of PNA to DNA), and 50% inhibition at ~0.45 μM (17:1 ratio). The anomalous migration of the 110-bp fragment (Fig. 1B, lanes 3 to 7) was due to bound PNA (*13*).

Nonspecific inhibition of Hind III by the PNA was monitored by examining cleavage at a second Hind III site 10 bp away from the $A_{10} \cdot T_{10}$ sequence (*10*). Even at 1 μM PNA T_{10}Lys, no inhibition of Hind III cleavage at this Hind III site was observed (Fig. 1C).

Strand invasion by PNA T_{10}Lys was salt-dependent. If the PNA and DNA were preincubated in Hind III reaction buffer (50 mM tris, 50 mM NaCl, 10 mM $MgCl_2$), in place of a low-salt buffer (*12*), 10 to 20% strand invasion was observed at a 1 μM PNA dose. Thus, PNA strand invasion may require DNA breathing.

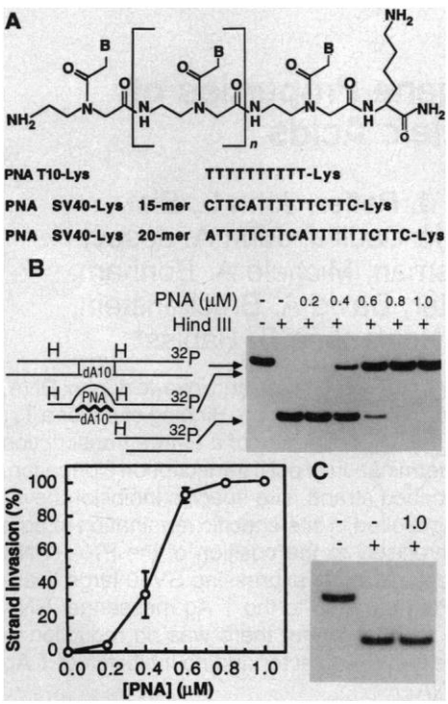

Fig. 1. (**A**) Structure of a PNA, and PNA oligomer sequences. (**B**) Detection of a PNA · DNA complex by inhibition of Hind III cleavage at a site overlapping the PNA $dA_{10} \cdot T_{10}$ target. Shown on the left are the schematic structures describing each band. Lanes are described in the text as 1 to 7 reading left to right. H is Hind III. The strand invasion (% inhibition of Hind III cleavage) versus [PNA] is also indicated. The points are the mean of four experiments and are shown with standard deviation error bars. (**C**) Effect of PNA T_{10}Lys on Hind III cleavage of a Hind III site not overlapping the $dA_{10} \cdot T_{10}$ target.

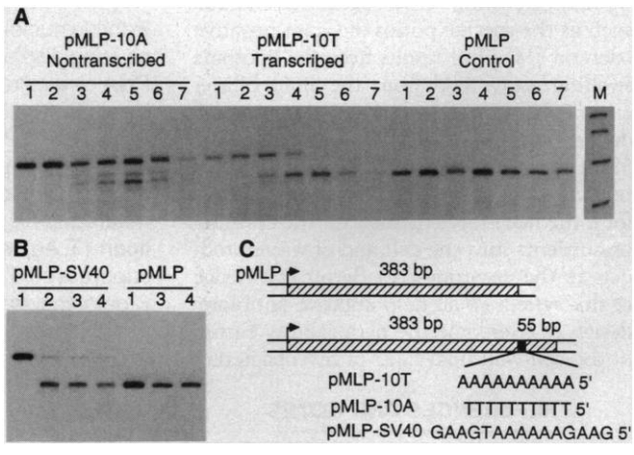

Fig. 2. Site-specific inhibition of pol II transcription elongation. (**A**) Strand invasion and inhibition of transcription by T_{10}Lys. Three plasmids containing a G-free cassette sequence and either no insert (pMLP), the dA_{10} target on the nontranscribed strand (pMLP-10A), or the dA_{10} on the transcribed strand (pMLP-10T) were used in the transcription reactions; T_{10}Lys concentrations for lanes 1 to 7 are, respectively, 0, 0.25, 0.5, 0.75, 1, 2, and 3 μM. The size of the full-length transcripts for pMLP-10T and pMLP-10A is 448 bases, and for pMLP is 383 bases. The size markers (lane M) are 628, 532, 401, and 311 bases. (**B**) Strand invasion and inhibition of transcription by the SV40 15-mer PNA with the plasmids pMLP (no insert) and pMLP-SV40 (containing an SV40 target sequence on the transcribed strand). The full-length transcript for pMLP-SV40 is 448 bases. T_{10} Lys concentrations for lanes 1 to 4 are, respectively 0, 1, 2, and sum. (**C**) Schematic of pMLP plasmids showing the relative location of G-free cassette sequence (diagonal lines) and the PNA target sequences (black box). The nucleotide sequence of the transcribed (bottom) strand for each target-containing plasmid is shown. The arrow indicates the direction of transcription from the major late promoter.

The Hind III inhibition assay was also used to assess the rate of D-loop formation. When 1 μM T_{10}Lys was preincubated with the Bss HII–Kpn I restriction fragment prior to the addition of Hind III, ~20 min was required for complete strand invasion. Nielsen *et al.* (*7*) observed similar strand invasion kinetics with $KMnO_4$ hyperreactivity of the DNA in the presence of PNA.

The strand-invading capability of the PNA suggested that it could be used in an antigene strategy in vitro by disrupting transcription elongation. A $dA_{10} \cdot T_{10}$ target sequence was localized downstream of a G-free transcription cassette in the pMLP plasmid vector (*14*), which uses the adenovirus major late promoter to drive transcription. We could then examine PNA-dependent transcription termination with the dA_{10} target on either the transcribed or nontranscribed strand. In addition, an SV40 T antigen sequence was cloned into the transcribed strand of pMLP (*14*). The pMLP transcription vectors (Fig. 2C) would yield expected transcripts of 383 bases for pMLP and 448 bases for pMLP-10T (dA_{10} on the transcribed strand), pMLP-10A (dA_{10} on the nontranscribed strand), and pMLP-SV40. Site-specific termination of transcription should result in a truncated transcript of 388 bases from plasmids containing the inserts (Fig. 2).

The plasmids were preincubated with various concentrations of T_{10}Lys or a 15-mer SV40 PNA (Fig. 1A) to allow D-loop formation. Transcription was initiated by using a rat liver or Hela cell nuclear extract as the source of transcription factors (*15–17*). As shown in Fig. 2, A and B (lanes marked pMLP), and in additional studies, PNA concentrations up to 1 μM did not influence the transcriptional signal of pMLP. However, higher concentrations of PNA gave some nonspecific inhibition of the 383-base transcript.

The use of pMLP-10T, which targets the PNA to the strand the polymerase is reading, led to a dose-dependent loss of the full-length transcript band of 448 bases and the formation of a new 388-base transcript, which truncated precisely at the $dA_{10} \cdot T_{10}$ site (Fig. 2A, lanes marked pMLP-10T). At a concentration of 1 μM T_{10}Lys, 100% inhibition of pol II elongation was observed, with 50% inhibition seen between 0.5 and 0.75 μM. This dose dependence was similar to that for PNA-dependent inhibition of Hind III cleavage (Fig. 1B). Unlike inhibition of pol II transcription by triplex formation, which has been shown to be transient because of the instability of the ODN · DNA complex (*3*), the inhibition we observed persisted for at least 1 hour.

The use of pMLP-10A, which targets the PNA to the nontranscribed strand, led to only partial inhibition of transcription, even at 1 μM T_{10}Lys (Fig. 2A, lanes marked pMLP-10A). A transcript of ~410 bases was also observed, although its presence was not reproducible.

Fig. 3. Site-specific inhibition of RT by T_{10}Lys (micromolar concentrations given above the lanes). For the A_{10}-containing RNA, the cDNA that terminates at the A_{10} was 109 bases, and the full-length cDNA was 198 bases. For the U_{10}-containing RNA, the U_{10} was 129 bases, and the full-length cDNA was 204 bases. The line drawings show the position of the full-length cDNAs and the A_{10} or U_{10} sequence on the gel. The starting position of cDNA synthesis, or the portion of the RNA upstream of initiation, are not shown to scale.

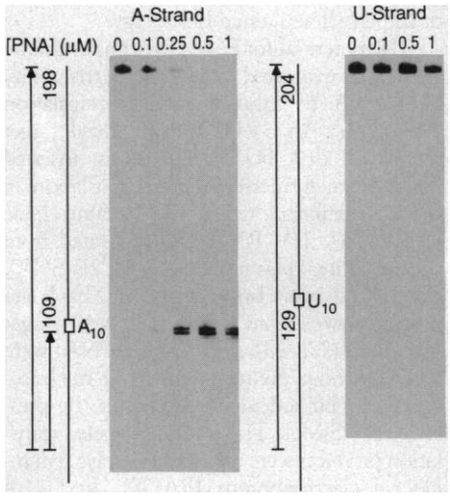

Strand invasion by a PNA was not restricted to $A_n \cdot T_n$ sequences. We cloned an SV40 T antigen sequence into the G-free transcription cassette, forming pMLP-SV40, and prepared a 15-mer PNA (Fig. 1A) that was complementary to the transcribed strand of the SV40 sequence. At 1 μM 15-mer PNA, there was a significant reduction of the full-length transcript from pMLP-SV40, and formation of a transcript truncated at the SV40 sequence (Fig. 2B). The ability of a PNA to strand invade duplex DNA may be restricted to A-T–rich domains, as the SV40 target sequence is 73% A-T.

With their high avidity for DNA, we assumed that PNAs would also bind RNA. We evaluated the ability of T_{10}Lys to form a heteroduplex with RNA and thereby inhibit RT progression. The phage T3 promoter on pBSA10 was used to synthesize a 268-base RNA transcript containing an rA_{10} target sequence for T_{10}Lys (*18*). After incubation of this RNA with T_{10}Lys (and a primer to initiate RT), cDNA synthesis was performed with RNase H^- MMLV reverse transcriptase (*19*). As shown in Fig. 3 (A-strand panel), increasing amounts of PNA T_{10}Lys resulted in a dose-dependent loss of the full-length cDNA 198-base band (with complete loss at 0.5 μM PNA) and in the appearance of a set of bands ~109 bases in length, corresponding to the rA_{10} site. No other PNA-dependent termination products were observed. Reverse transcription of pBSA10 RNA synthesized from the T7 promoter (containing the complementary U_{10} sequence) (*18*) gave no premature termination of cDNA synthesis, even at 1 μM PNA (Fig. 3, U-strand panel). T_{10}Lys bound to rA_{10} site specifically and was able to terminate RT elongation. When a T_{10} ODN was used in the assay, no inhibition of RT was observed. A PNA, unlike ODNs (*5*), can inhibit elongation of RT in an RNase H–independent manner because of the highly stable nature of the RNA · PNA heteroduplex.

Preincubation of the PNA with the RNA was performed in RT reaction buffer (*19*), and not in the low-salt buffer used in the strand invasion experiments. Efficient binding of a PNA to RNA does not require low salt, presumably because the PNA binding site within the RNA remains single-stranded in the reaction buffer.

By using the 15-mer SV40 PNA, and RNA containing its binding site, sequence-specific inhibition of RT was observed. As with DNA, the binding of PNAs to RNA is not restricted to $A_n \cdot T_n$ sequences. However, when T_{10}Lys was incubated with RNA containing the SV40 site, inhibition of RT was observed at a sequence (GAA-GAAAAAA) containing two mismatched PNA · RNA base pairs. Therefore the binding of PNA to RNA can occur at sites

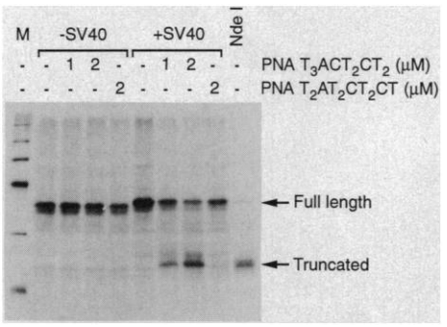

Fig. 4. Site-specific inhibition of in vitro translation. RNAs with or without the SV40 T antigen–derived target sequence for the PNA were prepared from pGEM-IL2R-SV40 and pGEM-IL2R3, respectively, and translated with a rabbit reticulocyte lysate. Full-length translation products and those truncated at the SV40 target site are shown by arrows. The +SV40 full-length translation product was slightly larger because of insertion of the PNA target sequence into the IL2R cDNA. The lane marked Nde I is the translation product of RNA prepared from pGEM-IL2R3 cleaved at Nde I (the site into which the SV40 insert was cloned). The molecular masses of the marker lane (M) are 200, 97.4, 68, 43, 29, and 18.4 kD.

of imperfect sequence homology.

The potential for PNAs to act as antisense agents was evaluated by examining the ability of a PNA to inhibit in vitro translation elongation. An SV40 T Ag–derived target sequence, $d(A_3TGA_2GA_2)$, was inserted downstream from the start of translation of the interleukin-2 receptor α subunit gene cDNA (*20, 21*). RNA was generated from the resulting plasmid, pGEM-IL2R-SV40, which had been linearized at a Xba I site further downstream than the SV40 target sequence (*22, 23*). RNA and PNA were added without preincubation to a nuclease-treated rabbit reticulocyte lysate in the presence of [^{35}S]Met. The resulting labeled translation products were analyzed by polyacrylamide gel electrophoresis (PAGE). In Fig. 4 (+SV40 panel), we show that in the presence of PNA $T_3ACT_2CT_2$, there was a dose-dependent loss of the full-length 36-kD protein product and formation of a truncated 22-kD product, which corresponds to termination at the target site in the RNA (lane marked Nde I). Formation of the 22-kD product was dependent on the presence of the SV40 target site in the RNA (Fig. 4, −SV40 panel), and the amount of this product was greatly reduced when a scrambled PNA control sequence ($T_2AT_2CT_2CT$) was used. Translation inhibition was also seen when PNA T_{10}Lys, and an RNA containing an rA_{10} target, was used. In other experiments, we determined that a PNA · RNA heteroduplex was not a substrate for RNase H, and thus the translation termination we observed was not due to RNase H. In comparable studies, ODN analogs such as methylphosphonates and alpha ODNs were unable to block ribosome elongation (*6*).

We assessed the in vivo antisense-antigene potential of PNAs by cell microinjection. The ability of microinjected PNAs to block SV40 T Ag expression was examined with the temperature-sensitive tsa 8 cell line (*24*), which contains a single-copy integrant of the SV40 early region. Prior to microinjection, cells were maintained at the nonpermissive temperature (39°C) for a period of 48 hours to reduce T Ag protein to a nondetectable level (*24*) as assessed by indirect immunocytochemistry and protein immunoblotting. After microinjection, cells were shifted to the permissive temperature (33°C) and a PNA-dependent block of the reemergence of nascent T Ag protein synthesis was determined by indirect immunocytochemistry (*25*). To account for both nonspecific PNA effects and for cell viability after injection, a β-galactosidase (β-gal) expression vector was included in all microinjections. The percentage of β-gal–expressing cells that exhibited nuclear T Ag staining significantly weaker than that observed in noninjected cells in the same field was determined. This value was then corrected for the percentage of noninjected cells that failed to reexpress T Ag, giving us the PNA-specific percent inhibition.

The photomicrographs shown in Fig. 5 emphasize features typical of this assay. Cells microinjected with an antisense 20-mer SV40 PNA (Fig. 1) (intracellular concentration of ~1 μM) showed a significant reduction in T Ag expression (Fig. 5A, arrow). The specificity of this inhibition was confirmed by demonstrating a strong cellular staining pattern for exogenously expressed β-gal protein (Fig. 5B, arrow). In addition, Fig. 5, A and B (arrowhead), shows a cell that maintained a high level of both T Ag and β-gal expression, even though this cell presumably received a similar PNA dose. The extent and specificity of inhibition observed was dependent upon the concentration of PNA microinjected. Intracellular PNA concentrations exceeding 5 μM generally resulted in nonspecific inhibition of β-gal expression.

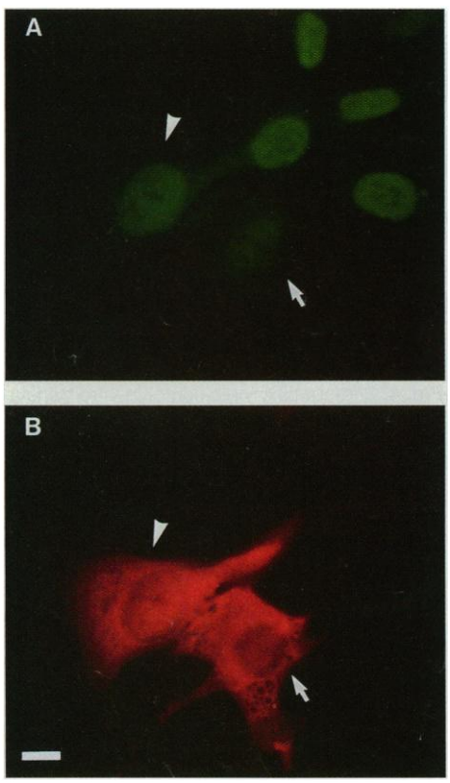

Fig. 5. Inhibition of T antigen expression in vivo. Tsa 8 cells were maintained at 39°C for 48 hours prior to microinjection of PNA 20-mer and a β-gal–expressing plasmid. Cells were then shifted to 33°C for 18 hours and processed for immunocytochemistry. (**A**) T antigen detection with fluorescein-conjugated secondary and tertiary antibodies. Following incubation at the permissive temperature, the majority of noninjected cells expressed detectable levels of nuclear-associated T Ag. Microinjection of PNA 20-mer (1 μM estimated intracellular concentration) resulted in a significant reduction in T Ag levels (arrow). Another injected cell (arrowhead) continued to express T Ag. (**B**) Detection of β-gal with a Texas red–conjugated secondary antibody. Two cells exhibited characteristic cytoplasmic staining. Nuclei were typically dark. Calibration bar, 15 μm.

When the 15-mer SV40 PNA was used, ~40% of the injected β-gal–expressing cells showed significantly reduced T Ag staining at an estimated concentration of 1 μM PNA per injected cell. The 20-mer PNA effected 50% inhibition at the same dose. In contrast, a 10-mer SV40 PNA ($CTTCT_6$Lys) was not capable of inhibiting T Ag reemergence at doses ranging from 1 to 10 μM. We conclude that both 15-mer and 20-mer PNAs directed against the SV40 large T Ag mRNA can effect inhibition of T Ag gene expression. Under similar experimental conditions, a 19-mer unmodified ODN targeted to the same SV40 T Ag sequence was not able to inhibit T Ag expression to any extent.

We have not yet addressed the mechanism by which PNAs are able to exert their effects on T Ag expression. Both DNA and RNA binding are possible, so suppression could occur at the level of transcription or translation. However, intranuclear salt concentration could preclude efficient strand invasion of the SV40 duplex DNA target by both the 15-mer and 20-mer PNAs. Therefore an antisense model of inhibition by PNAs would appear to be more likely. Additional studies using cell permeable PNAs or microinjected PNAs targeted to intronic regions are needed to distinguish between these two mechanisms.

REFERENCES AND NOTES

1. L. Neckers, L. Whitesell, A. Rosolen, D. A. Geselowitz, in *Critical Reviews in Oncogenesis* (CRC Press, Boca Raton, FL 1992), vol. 3, pp. 175–231; E. Wickstrom, Ed., *Prospects for Antisense Nucleic Acid Therapy of Cancer and AIDS* (Wiley-Liss, New York, 1991).
2. L. J. Maher III, B. Wold, P. B. Dervan, *Science* **245**, 725 (1989); J.-C. Francois, T. Saison-Behmoaras, N. T. Thuong, C. Helene, *Biochemistry* **28**, 9617 (1989); J. C. Hanvey, M. Shimizu, R. D. Wells, *Nucleic Acids Res.* **18**, 157 (1990); L. J. Maher, P. B. Dervan, B. Wold, *Biochemistry* **29**, 8820 (1990).
3. S. L. Young, S. H. Krawczyk, M. D. Matteucci, J. J. Toole, *Proc. Natl. Acad. Sci. U.S.A.* **88**, 10023 (1991).
4. G. Duval-Valentin, N. T. Thuong, C. Helene, *ibid.* **89**, 504 (1992).
5. C. Boiziau, N. T. Thuong, J.-J. Toulme, *ibid.*, p. 768.
6. R. Y. Walder and J. A. Walder, *ibid.* **85**, 5011 (1988); C. Cazenave *et al.*, *Nucleic Acids Res.* **17**, 4255 (1989); C. Boiziau *et al.*, *ibid.* **19**, 1113 (1991).
7. P. E. Nielsen, M. Egholm, R. H. Berg, O. Buchardt, *Science* **254**, 1497 (1991).
8. M. Egholm, O. Buchardt, P. E. Nielsen, R. H. Berg, *J. Am. Chem. Soc.* **114**, 1895 (1992).
9. PNAs were synthesized essentially as described in (*7, 8*).
10. The plasmid pBSA10, containing a $dA_{10} \cdot T_{10}$ target sequence for PNA T_{10}Lys, was constructed by cloning a 62-bp duplex into the Hind III and

Xba I sites of pBluescript II KS+. To monitor Hind III cleavage at the site that overlaps the $dA_{10} \cdot T_{10}$ sequence, pBSA10 was cleaved with Bss HII, end-labeled with Klenow and [α-^{32}P]dCTP, and then cleaved with Kpn I. The 156-bp fragment was purified by polyacrylamide gel electrophoresis (PAGE). To detect Hind III cleavage at the Hind III site that does not overlap the $dA_{10} \cdot T_{10}$ site, pBSA10 was digested with Bss HII, end-labeled as above, digested with Sst I, and the 167-bp fragment was purified by PAGE.

11. In some experiments, a small amount of S1 nuclease cleavage was seen on the A strand that mapped to the 3′ end of the dA_{10} sequence. This reactivity may reflect a slightly strained conformation in the phosphodiester backbone at the junction between the D-loop and double-stranded DNA.
12. PNA · DNA complexes for probing by Hind III were prepared by mixing 0.02 pmol (~40,000 cpm) of the pBSA10 restriction fragment (*10*) plus 0.5 pmol of Sst I linearized pBSA10 and incubating with various concentrations of T_{10}Lys in 1 mM tris, pH 8.0, and 0.1 mM EDTA for 1 hour at 37°C. After the addition of Hind III reaction buffer (50 mM tris, pH 8.0, 10 mM $MgCl_2$, and 50 mM NaCl) and 10 U (1 μl) of Hind III, the reactions (final volume 20 μl) were incubated for 1 hour at 37°C and terminated by the addition of 4 μl of 100 mM EDTA. The reaction products were analyzed by a 5% PAGE, and the bands were visualized by autoradiography. The relative amount of radioactivity in each band was determined with a Molecular Dynamics PhosphorImager. The percent strand invasion (percent inhibition of Hind III cleavage at the Hind III site overlapping the $dA_{10} \cdot T_{10}$ sequence) was calculated as the percentage of counts in the upper band divided by the total counts of the two bands.
13. We expected that T_{10}Lys, once bound to the DNA, would not dissociate during electrophoresis. Hind III reactions (*12*) were heated to 90°C in the presence of oligomer dA_{12} (20-fold molar excess of dA_{12} to PNA), and gradually cooled to 25°C. Subsequent PAGE revealed that the Hind III–cleaved restriction fragment migrated at the expected location of 110 bp.
14. The plasmids pMLP-10T and pMLP-10A were constructed by cloning a 64-bp fragment, with a dA_{10} sequence on either the transcribed or nontranscribed strand, respectively, into the Sma I and Hind III sites of pMLP (*16*). The plasmid pMLP-SV40 was constructed as above except that a 20-bp SV40 T antigen sequence (5′-GAAGAAAAAATGAAGAAAAT) was placed on the transcribed strand.
15. For in vitro transcription reactions with the T_{10}Lys, DNA · PNA complexes were formed by combining 0 to 60 pmol of PNA with 0.09 pmol (0.2 μg) of pMLP plasmid plus 0.39 pmol (0.8 μg) of promotor-minus plasmid (*16*) in 1 mM tris, pH 8.0, and 0.1 mM EDTA and incubating for 1 hour at 37°C in a total volume of 9 μl. In vitro transcription was initiated as described (*17*) with 4 μl of a rat hepatocyte nuclear extract in a total volume of 20 μl and incubated at 30°C for 40 min. For in vitro transcription reactions with the SV40 15-mer PNA, 0 to 150 pmol of PNA were incubated with 0.09 pmol (0.2 μg) of pMLP plasmid in 1 mM tris, pH 8.0, and 0.1 mM EDTA for 1 hour at 37°C in a total volume of 9 μl. In vitro transcription was initiated as described (*16*) with 3 μl of a HeLa nuclear extract (Promega) in a total volume of 25 μl and incubated at 30°C for 40 min. [^{32}P]UTP RNA transcripts were analyzed by 5 to 6% denaturing PAGE.
16. M. Sawadogo and R. G. Roeder, *Proc. Natl. Acad. Sci. U.S.A.* **82**, 4394 (1985).
17. K. Gorski, M. Carneiro, U. Schibler, *Cell* **47**, 767 (1986).
18. RNA containing the rA_{10} sequence was obtained by incubating 2 μg of Pvu II–linearized pBSA10 with 0.4 mM ribonucleotide 5′-triphosphates, 30 mM dithiothreitol (DTT), 80 U of RNasin, and 20 U of T3 RNA polymerase in T3/T7 buffer (40 mM tris, pH 7.5, 50 mM NaCl, 8 mM $MgCl_2$, and 2 mM spermidine) for 30 min at 37°C. Deoxyribonuclease I was added, followed by phenol-chloroform extraction and ethanol precipitation. RNA containing the U_{10} sequence was obtained as above, except that T7 RNA polymerase was used.
19. RNA · ODN primer complexes for RT were prepared by combining 0.5 μg of RNA (*18*) and 125 ng of ODN (M13-20 primer or reverse primer) to a final volume of 10 μl, heating to 70°C for 10 min, and then placing the solution on ice. Hybridization of PNA to the RNA · ODN mixtures was performed at 37°C by the addition of 1 μl of PNA (0 to 1 μM final concentrations), 4 μl of 5× buffer (250 mM tris, pH 8.3, 375 mM KCl, and 15 mM $MgCl_2$), 2 μl of 100 mM DTT, and 1 μl (40 U) of RNasin. After 20 min, 1 μl of a solution of deoxyribonucleotide 5′-triphosphates (dNTPs) {10 mM of dGTP, TTP, and dCTP, 0.1 mM dATP, and 10 μCi of [α-^{32}P]dATP} was added and the reaction initiated by the addition of 1 μl (200 U) of Superscript RNase H$^-$ MMLV reverse transcriptase (BRL). After a 15-min incubation, 1 μl of 10 mM dATP was added and after an additional 15 min the reaction was terminated by 4 μl of 0.5 M EDTA, phenol-chloroform extraction, and ethanol precipitation. The samples were analyzed by 6% denaturing PAGE.
20. Plasmid pGEM-IL2R-SV40, containing a $d(A_3TGA_2GA_2)$ segment on the coding strand, was constructed by cloning a 33-bp duplex into the Nde I site of pGEM-IL2R3 (gift of W. C. Greene) (*21*).
21. W. J. Leonard *et al.*, *Nature* **311**, 626 (1984).
22. RNA for in vitro translation was prepared from Xba I–digested pGEM-IL2R3, Xba I–digested pGEM-IL2R-SV40, or Nde I–digested pGEM-IL2R3 as previously described (*23*). RNA (0.5 μg) and PNA (0 to 50 pmol) were mixed on ice with 20 μM amino acid mixture (minus Met), 2 mM DTT, 20 U of RNasin, 80 mM KCl, 1 μl of [^{35}S]Met (1100 Ci/mmol, 10 mCi/ml), and 16.5 μl Promega Flexi Rabbit Reticulocyte Lysate in a total reaction volume of 25 μl. Incubations were performed at 30°C for 1 hour and were terminated by boiling for 3 min in 62.5 mM tris-HCl, pH 6.8, 10% glycerol, 2% SDS, and 5% β-mercaptoethanol. The samples were analyzed by 12% SDS-PAGE.
23. D. E. Titus, Ed., *Promega Protocols and Applications Guide* (Promega, Madison, WI, ed. 2, 1991), pp. 59–61.
24. P. S. Jat and P. A. Sharp, *Mol. Cell. Biol.* **9**, 1672 (1989).
25. Tsa8 cells were maintained in Dulbecco modified Eagle medium supplemented with 10% fetal calf serum, penicillin, and G418 (0.33 mg/ml). For microinjection studies, cells were plated onto Nunc two-chamber glass slides and incubated at 33°C for 24 hours. Prior to microinjection, cells were maintained at 39°C for 48 hours Microinjection was performed at room temperature with phenol red–free medium containing 25 mM Hepes. Plasmid (final concentration 0.16 μg/ml) and PNAs were prepared in 80 mM KCl and 50 mM Hepes (pH 7 3). Nuclear injection volumes of 10×10^{-15} to 20×10^{-15} liters resulted in ~200 copies of plasmid per nucleus and a 1:20 dilution of PNA (assuming a cell volume of 400×10^{-15} liters). Microinjection was performed with a Zeiss Axiovert 35M inverted microscope and the Zeiss AIS microinjection system. The protocol for indirect fluorescent immunocytochemical detection of T Ag and β-gal was developed by R. Wagner (Gilead Sciences, Foster City, CA) All steps were performed at room temperature. Cells were fixed for 15 min in 3.7% formalin and permeabilized with 1.0% NP-40. T Ag was detected with a primary mouse monoclonal antibody (PharMingen) and fluorescein-conjugated secondary and tertiary antibodies (sheep antibody to mouse and donkey antibody to sheep, Jackson Immunoresearch Laboratories). β-Galactosidase was detected with a primary rabbit antibody (5 Prime–3 Prime, Inc.) and a Texas red–conjugated secondary donkey antibody to rabbit (Jackson Immunoresearch Laboratories). All antibodies were diluted 1:100 in the BSA-blocking buffer and incubated for 45 min. Immunocytochemistry was examined with a Zeiss Axiovert 35M microscope (40×, 0.60 phase-contrast objective) equipped with an epifluorescence illumination system [fluorescein filters (450–490/FT 510/LP 520); Texas red filters (BP 546/FT 580, LP 590)]. Epifluorescence photomicroscopy was performed on a Nikon Optiphot (40× oil, 1.30) with fluorescein (B1-E) and Texas red (G2-B) filter cubes. Photomicrographs were obtained from Kodak Ektachrome 400 film.

14 August 1992; accepted 21 September 1992

Dual-Target Inhibition of HIV-1 in Vitro by Means of an Adeno-Associated Virus Antisense Vector

Saswati Chatterjee,* Philip R. Johnson,† K. K. Wong, Jr.‡

An adeno-associated virus vector encoding an antisense RNA was used to transduce stable intracellular resistance to human immunodeficiency virus–1 (HIV-1) in human hemopoietic and non-hemopoietic cell lines. The antisense targets are present in all HIV-1 transcripts and include the TAR sequence, which is critical for transcription and virus replication, and the polyadenylation signal. Cell lines expressing antisense RNA showed up to 95 percent inhibition of gene expression directed by the HIV-1 long terminal repeat and greater than 99 percent reduction in infectious HIV-1 production, with no detectable cellular toxicity. Because of their efficient transcription and inability to recombine with HIV-1, adeno-associated virus vectors represent a promising form of anti-retroviral gene therapy.

Current estimates indicate that more than 1 million people in the United States may be infected with HIV-1, a causative agent of acquired immunodeficiency syndrome (AIDS) (*1*). One potential form of gene therapy for AIDS is based on the concept of intracellular immunization, the induced expression of molecules that block HIV gene transcription or translation (*2*). Molecules with potential HIV inhibitory activity include the trans-dominant proteins derived from viral *rev* (*3*) and *gag* genes (*4*) and ribozymes targeted to transcripts of the *gag* (*5*) and integrase genes (*6*) and to the 5′ leader RNA (*7*). Antisense RNAs may also be used to block HIV-1 infection, although the success of this approach thus far has been limited by inefficient expression and poor target selectivity (*8*). In many of these experiments, the antisense RNAs were ex-